



AFRL-RX-WP-TP-2014-0022

**BISMALEIMIDE/PRE-CERAMIC POLYMER BLENDS
FOR HYBRID MATERIAL TRANSITION REGIONS:
PART 1. PROCESSING AND CHARACTERIZATION
(POSTPRINT)**

**Vernon T. Bechel, Janis M. Brown, and Marilyn R. Unroe
AFRL/RXCC**

**Sirina Safriet
University of Dayton Research Institute**

**JANUARY 2014
Interim Report**

Approved for public release; distribution unlimited.

See additional restrictions described on inside pages

STINFO COPY

© 2012 Sage Publication

**AIR FORCE RESEARCH LABORATORY
MATERIALS AND MANUFACTURING DIRECTORATE
WRIGHT-PATTERSON AIR FORCE BASE, OH 45433-7750
AIR FORCE MATERIEL COMMAND
UNITED STATES AIR FORCE**

NOTICE AND SIGNATURE PAGE

Using Government drawings, specifications, or other data included in this document for any purpose other than Government procurement does not in any way obligate the U.S. Government. The fact that the Government formulated or supplied the drawings, specifications, or other data does not license the holder or any other person or corporation; or convey any rights or permission to manufacture, use, or sell any patented invention that may relate to them.

This report was cleared for public release by the USAF 88th Air Base Wing (88 ABW) Public Affairs Office (PAO) and is available to the general public, including foreign nationals.

Copies may be obtained from the Defense Technical Information Center (DTIC) (<http://www.dtic.mil>).

AFRL-RX-WP-TP-2014-0022 HAS BEEN REVIEWED AND IS APPROVED FOR PUBLICATION IN ACCORDANCE WITH ASSIGNED DISTRIBUTION STATEMENT.

//Signature//

MARILYN R. UNROE, Project Engineer
Composites Branch
Structural Materials Division

//Signature//

DONNA L. BALLARD, Deputy Chief
Composites Branch
Structural Materials Division

//Signature//

ROBERT T. MARSHALL, Deputy Chief
Structural Materials Division
Materials and Manufacturing Directorate

This report is published in the interest of scientific and technical information exchange, and its publication does not constitute the Government's approval or disapproval of its ideas or findings.

REPORT DOCUMENTATION PAGE			Form Approved OMB No. 0704-0188		
The public reporting burden for this collection of information is estimated to average 1 hour per response, including the time for reviewing instructions, searching existing data sources, gathering and maintaining the data needed, and completing and reviewing the collection of information. Send comments regarding this burden estimate or any other aspect of this collection of information, including suggestions for reducing this burden, to Department of Defense, Washington Headquarters Services, Directorate for Information Operations and Reports (0704-0188), 1215 Jefferson Davis Highway, Suite 1204, Arlington, VA 22202-4302. Respondents should be aware that notwithstanding any other provision of law, no person shall be subject to any penalty for failing to comply with a collection of information if it does not display a currently valid OMB control number. PLEASE DO NOT RETURN YOUR FORM TO THE ABOVE ADDRESS.					
1. REPORT DATE (DD-MM-YY) January 2014		2. REPORT TYPE Interim		3. DATES COVERED (From - To) 01 October 2008- 30 September 2012	
4. TITLE AND SUBTITLE BISMALEIMIDE/PRECEMIC POLYMER BLENDS FOR HYBRID MATERIAL TRANSITION REGIONS: PART 1. PROCESSING AND CHARACTERIZATION (POSTPRINT)			5a. CONTRACT NUMBER In-house		
			5b. GRANT NUMBER		
			5c. PROGRAM ELEMENT NUMBER 62102F		
6. AUTHOR(S) Vernon T. Bechel, Janis M. Brown, and Marilyn R. Unroe (AFRL/RXCC) Sirina Safriet (University of Dayton Research Institute)			5d. PROJECT NUMBER 4347		
			5e. TASK NUMBER		
			5f. WORK UNIT NUMBER XOBP		
7. PERFORMING ORGANIZATION NAME(S) AND ADDRESS(ES) AFRL/RXCC 2941 Hobson Way Wright-Patterson AFB, OH 45433			8. PERFORMING ORGANIZATION REPORT NUMBER		
University of Dayton Research Institute 300 College Park Drive Dayton, OH 45469					
9. SPONSORING/MONITORING AGENCY NAME(S) AND ADDRESS(ES) Air Force Research Laboratory Materials and Manufacturing Directorate Wright-Patterson Air Force Base, OH 45433-7750 Air Force Materiel Command United States Air Force			10. SPONSORING/MONITORING AGENCY ACRONYM(S) AFRL/RXCC		
			11. SPONSORING/MONITORING AGENCY REPORT NUMBER(S) AFRL-RX-WP-TP-2014-0022		
12. DISTRIBUTION/AVAILABILITY STATEMENT Approved for public release; distribution unlimited.					
13. SUPPLEMENTARY NOTES PA Case Number: 88ABW-2012-4313; Clearance Date: 08 Aug 2012. Journal article published in <i>High Performance Polymers</i> , 25(4), 363-376 (2013). © 2012 Sage Publication. The U.S. Government is joint author of the work and has the right to use, modify, reproduce, release, perform, display, or disclose the work. This paper contains color. The final publication is available at hip.sagepub.com . For additional information, see AFRL-RX-WP-TP-2014-0023 (Part 2).					
14. ABSTRACT (Maximum 200 words) Initial steps were taken in the study of processing mixtures of a polymer and a preceramic polymer to produce a hybrid material that contains a region of gradual transformation from a polymer to a ceramic. It is thought to be a first step toward the eventual development of a hybrid that is graded from a polymer matrix composite to a ceramic matrix composite. Thermal and elemental analysis, and morphology characterization of RD-730 preceramic polymer blends, which convert to silicon carbide upon pyrolysis, and Matrimid A/B polymer (a bismaleimide), were carried out as a function of cure cycle. Cure cycles were chosen to vary the resin viscosity during processing in order to affect the amount of phase separation observed. The results were then used to associate processing parameters with the miscibility of the two resins and the likelihood of producing a hybrid with mechanical and thermal properties that fall between those of the two constituents. High RD-730 loadings were achieved without phase inversion, the glass transition (T _g) of the blended material was shown to be significantly influenced by post-cure, and thermal gradients observed.					
15. SUBJECT TERMS hybrid material, composite material, polymer matrix composite, ceramic matrix composite, thermal protection system, preceramic polymer					
16. SECURITY CLASSIFICATION OF:			17. LIMITATION OF ABSTRACT: SAR	18. NUMBER OF PAGES 17	19a. NAME OF RESPONSIBLE PERSON (Monitor) Marilyn R. Unroe
a. REPORT Unclassified	b. ABSTRACT Unclassified	c. THIS PAGE Unclassified			19b. TELEPHONE NUMBER (Include Area Code) (937) 255-9071



Bismaleimide/preceramic polymer blends for hybrid material transition regions: Part I. Processing and characterization

High Performance Polymers
25(4) 363–376
© The Author(s) 2012
Reprints and permission:
sagepub.co.uk/journalsPermissions.nav
DOI: 10.1177/0954008312468351
hip.sagepub.com



Vernon T. Bechel¹, Sirina Safriet^{1,2}, Janis M. Brown¹ and Marilyn R. Unroe¹

Abstract

In this article, initial steps were taken in the study of processing mixtures of a polymer and a preceramic polymer to produce a hybrid material that contains a region of gradual transformation from a polymer to a ceramic. It is thought to be a first step toward the eventual development of a hybrid that is graded from a polymer matrix composite to a ceramic matrix composite. Thermal analysis, elemental analysis, and morphology characterization of blends of RD-730 preceramic polymer, which converts to silicon carbide upon pyrolyzation, and Matrimid A/B polymer which is a bismaleimide were carried out as a function of cure cycles. The cure cycles were chosen to vary the resin viscosity at specific times during processing in order to affect the amount of phase separation of the two resins. These results were then used to make conclusions on how processing parameters affected the miscibility of the two resins and the likelihood of producing a hybrid having mechanical and thermal properties that fall between those of the two constituents. High RD-730 loadings were achieved without phase inversion, the glass transition temperature (T_g) of the blended material was shown to be significantly influenced by a post-cure, and a spatial gradient in RD-730 concentration was noted.

Keywords

Preceramic polymer, hybrid, composite, thermal protection system

Introduction

Hybrid structures consisting of multiple material constituents with internal transitions between materials, which are a compact ‘morphing’ of one constituent to another (as opposed to an abrupt interface), have been studied for use in various applications,¹ such as high-temperature combustors and ceramic structures with tougher faces.^{2,3} Conceivably, this concept could be expanded to hybrids with a polymer matrix composite (PMC) constituent. A PMC could be given added functionality if it were possible to embed within it small regions made of ceramic or ceramic matrix composite (CMC). These embedded regions could be for wear resistance, chemical resistance, hard points for connectors, or added temperature capability in a component subject to a temperature gradient. In other cases, these embedded regions may simply need to be somewhat ‘ceramic-like’ in terms of stiffness and coefficient of thermal expansion (CTE) to enable an efficient transition with less severe stress concentrations to a neighboring ceramic structure.⁴ Figure 1

shows two examples of applications that could benefit from these PMC-to-ceramic graded regions.

Figure 1(a) shows a simplified schematic representation of a notional panel for an integrated thermal protection system. Conceptually, the panel experiences a large temperature gradient in flight with a higher temperature on the CMC layer facing the exterior of the vehicle and a lower temperature on the PMC layer facing the interior of the vehicle. This type of multilayer panel has been discussed in a general sense for future designs of atmospheric reentry vehicles and hypersonic transports. The design may require

¹ Air Force Research Laboratory, Wright Patterson AFB, OH, USA

² University of Dayton Research Institute, Dayton, OH, USA

Corresponding author:

Vernon T. Bechel, Air Force Research Laboratory, Wright Patterson AFB, OH 45433, USA.

Email: Vernon.Bechel@wpafb.af.mil

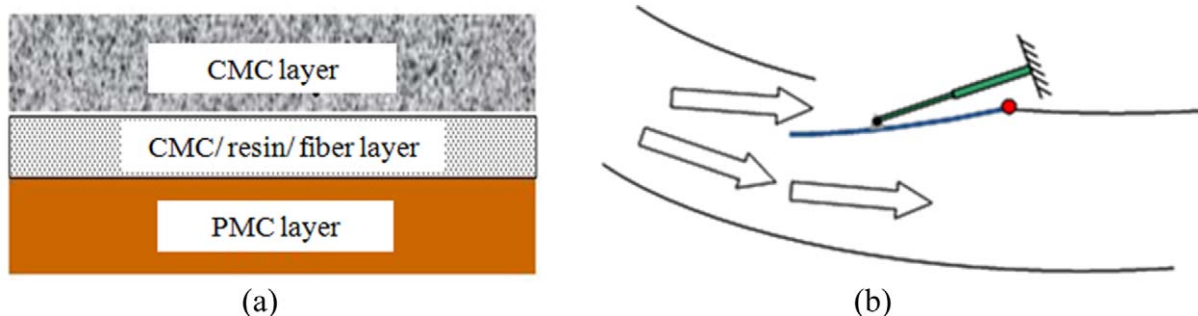


Figure 1. Hybrid material applications: (a) thermal protection and (b) valve opening into fluid stream.

the PMC and the CMC to be rigidly connected together in order that all layers share the mechanical loads.^{5,6} In that event, the transition region between the two must be sufficiently robust that it can sustain the stresses caused by the difference in mismatch in CTE between the PMC and CMC and it must bear the stresses caused by the temperature gradient through the panel thickness. Grading the transition region may reduce the stresses at the interfaces between the layers (and in this case, the graded region would also need to be designed for low-thermal diffusivity). Figure 1(b) shows a second notional application for this type of material. The figure represents a PMC door or valve surface that opens by moving into an air stream. The door is primarily made of PMC to take advantage of its specific strength and stiffness. However, the higher velocity of the fluid flow around the leading edge of the opened door causes higher temperatures near the leading edge, and abrasive particles in the fluid stream cause damage in the same leading edge area. A small embedded region of ceramic or CMC may be the best solution for the leading edge area. Ideally, it would grade from one material to the next to reduce local stress concentrations^{6,7} and the reinforcing fibers of the PMC would be continuous through the transition region for greater 'joint' strength. The work on the polymer/ceramic blends in this article was conducted to address some of the issues involved in processing a matrix that might be used in the graded regions for examples such as these.

Past work on nongraded approaches to polymer/ceramic hybrids included the addition of cured silicone preceramic materials, silicone copolymers, organic nano-layered silicates, and polyhedral oligomeric silsesquioxane to organic thermosetting resins. These additions were made to increase the operating temperatures, improve the thermo-oxidative stability, enhance the atomic oxygen resistance, and provide a barrier for diffusion of gas and liquid through a polymer. However, adding fillers frequently has limitations on the maximum loading that is possible. In a concept closer to the notion of a hybrid, a material was fabricated that comprised a layer of silicone matrix PMC co-cured in contact with a layer of traditional PMC and then post-cured in service. This early hybrid approach was successfully applied to a missile nosecone.^{8,9} The outer

non-PMC layer is converted to silica in situ upon exposure to high temperatures and oxygen in service.^{10,11} A gradient in properties through the thickness of the silica layer was the likely result, but the gradient between the two materials both in terms of chemistry and properties was not achieved in a controlled fashion, and this approach was only viable for a single-use application.

Techniques for combining a polymer and a ceramic are limited in number. If a ceramic powder is mixed with an uncured polymer, the cured material will simply be polymer with ceramic inclusions.¹² In such case, the CTE of the mixture may be between the CTE of the polymer and the ceramic powder. On the other hand, with the exception of molecular level approaches such as combining functionalized nanoparticles with the polymer, it is unlikely that the mixture would have a temperature capability greater than the polymer matrix. If instead of using a ceramic powder, a preceramic polymer is used, then both the polymer and preceramic are in an uncured, liquid form during mixing. In that case, it may be possible to control the processing conditions such that the preceramic polymer remains miscible or partially miscible in the polymer until mobility is sufficiently reduced to prevent significant phase separation. It is hypothesized that with this approach, there is the potential for a new material to be formed with a glass transition temperature (T_g) between the T_g of the polymer and the T_g of the preceramic polymer. This was the approach taken in the current work.

Experimental

Materials

Two materials had to be chosen for the polymer/preceramic polymer blends and ideally they would be representative of resins that would be used in the real applications similar to those shown in Figure 1. The polymer was chosen first based on three general characteristics: (1) processing parameters that would be as compatible as possible with the preceramic polymer, (2) a relatively high-service temperature, and (3) potential chemical suitability with the preceramic polymer. Then a bismaleimide (BMI) was chosen.

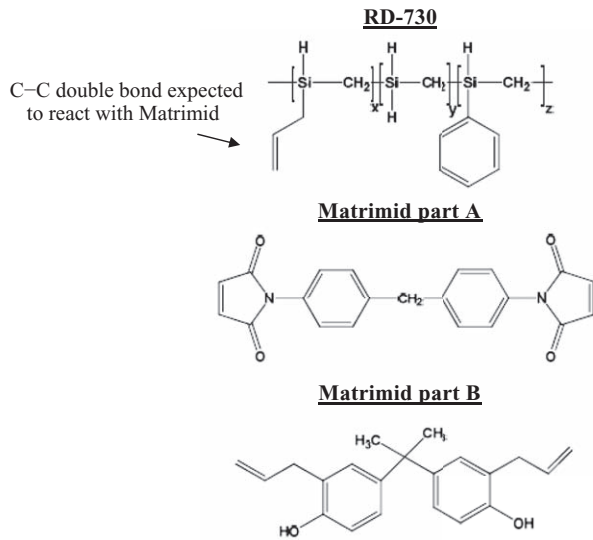


Figure 2. Chemical structures of RD-730 and Matrimid.

High-temperature BMIs now used in some PMCs are near the limits (for polymers) of T_g , thermo-oxidative stability, and processability using standard composite processing techniques. While their range of service temperatures is a long way from the processing temperatures required to convert preceramics to a ceramic, their flow and B-staging characteristics match well with a few preceramic materials making it possible to fabricate them together. Furthermore, for future work in which a dense fabric of reinforcement fibers is incorporated in the hybrid, composite-like processing of the silicon carbide (SiC) preceramic material used in this work was believed to be achievable in the range of 200°C–400°C, which was also a good range for BMIs. A final reason for choosing a BMI was that at around 150°C, it was expected that a silicon-based preceramic may potentially be reactive with the carbon-carbon double bond of the imide in the BMI. The BMI formulation chosen was Matrimid 5292 A/B purchased from Huntsman (Freeport, TX, USA). This two-part system comprised 4,4'-bismaleimido-diphenyl methane (component A) and *o,o'*-diallyl bisphenol A (DABA, component B). All chemicals were used as received. The chemical structures of RD-730 and Matrimid are shown in Figure 2.

Next the preceramic polymer was chosen. Preceramic polymers are organic-inorganic polymers whose backbone often contains Si atoms.^{13,14} They are transformed into a variety of ceramic materials through the elimination of organic moieties by breaking C-H bonds and by releasing H₂, CH₄, and other volatile compounds. This is accomplished either by heat (pyrolysis) or by a nonthermal process such as ion irradiation. Upon heating, they can be converted to silicon dioxide, silicon oxycarbide (SiOC), SiC, silicon carbon nitride, and many other chemical forms depending on their composition in the polymeric state and the processing

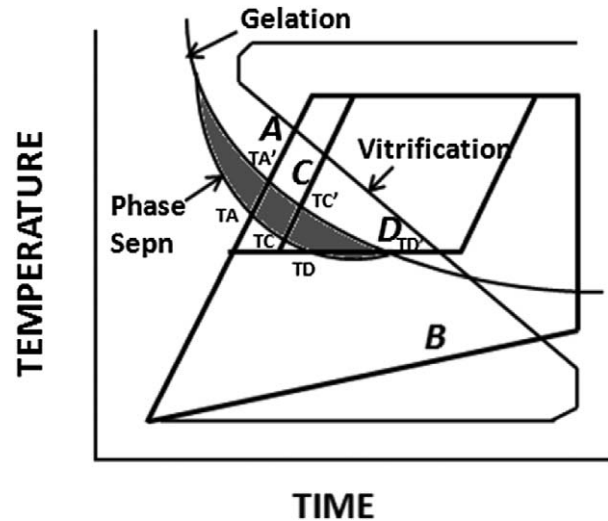


Figure 3. Typical time-temperature-transformation diagram (schematic) for a toughened thermosetting resin.

conditions used.^{15,16} The choice of ambient conditions (e.g. inert or oxidizing atmosphere) and maximum heating temperature are the key processing variables.^{17,18}

Allylhydridophenylpolycarbosilane – with trade name Starfire RD-730 from Starfire Systems (Schenectady, NY, USA) – was chosen for the preceramic polymer. It is a hot-melt material that is a precursor of thermally stable SiC. It is an inorganic resin that potentially has the temperature capability of a ceramic and the processing ease of organic polymers^{19–21} during casting or infusion in a reinforcing fiber network. It is curable to an intermediate at 150°C and, as stated, was also thought to be potentially reactive with the carbon-carbon double bond of the imide in a BMI. Therefore, it was a good candidate for studying the methodology of combining a polymer with a ceramic. Furthermore, in a previous article on preceramics for use in hybrids²², several aspects of the processing and characterization of RD-730 resin and a carbon fiber/RD-730 composite were demonstrated. In that article, it was shown that RD-730 could be processed with resin film infusion and autoclave cured at 800°C to produce a CMC (matrix likely a SiOC or other non-SiC intermediate). Composite panels of RD-730 with eight plies of T650-35 carbon fabric were fabricated and characterized for void and microcrack content to develop and improve upon a representative cure cycle. The processing successes that were established on RD-730 in that article gave credence to the possibility of using it in future PMC/CMC hybrids and were built upon in this article.

Cure cycle considerations

A detailed time-temperature-transformation (TTT) diagram of a resin is an important tool in the development of an optimal cure cycle in order to obtain a desired

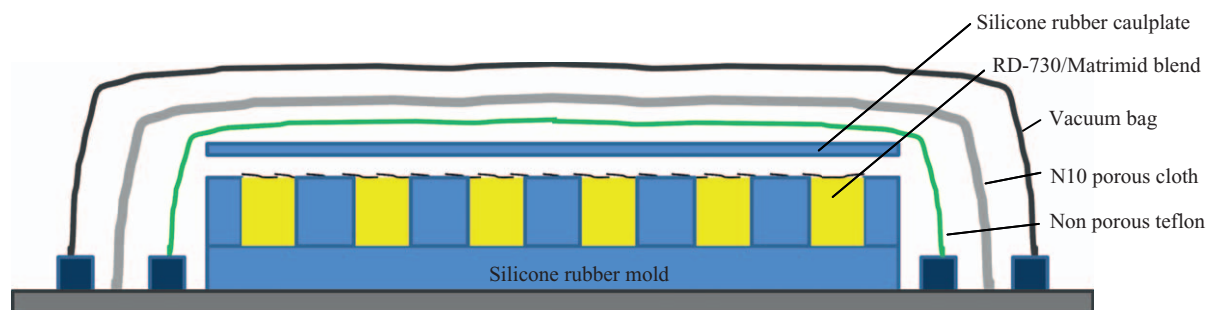


Figure 4. Schematic representation of sample setup.

morphology and set of properties.²³ Figure 3 shows a generic TTT diagram for toughened thermosetting resins.²¹ Four processing paths have been sketched on it as examples of cure cycles that eventually reach the same maximum temperature, but that can produce significantly different results. Path A cuts diagonally across the TTT diagram from a low temperature to a high temperature, allowing the phase separation to occur at relatively high temperatures. This has a tendency to yield a heterogeneous morphology since the resin can have a very low viscosity at the higher temperatures allowing ease of movement of disparate phases. Path B is a long shallow ramp that avoids the phase separation region entirely. The disadvantage of path B is that the temperatures along the slow ramp may be too low to activate a desired reaction (e.g. with another resin as is desired for our blended hybrid). Paths C and D are processing approaches that represent a compromise between the extremes of paths A and B. They balance the magnitude of the temperature during phase separation against the time spent at that temperature. The intent is to minimize the phase separation while maximizing the activation energy.

Unfortunately, a full TTT diagram was not available for RD-730 or Matrimid A/B to assist in developing cure cycles that could be tried to determine the optimum time for the RD-730 and Matrimid A/B to react while limiting the time that RD-730 had enough mobility to phase separation. Consequently, in this article, a best estimate on the basis of the work of Brown et al.²² was used to choose the parameters of two cure cycles that would represent extremes similar to paths A and D in Figure 3 that would work with RD-730. The objective was to study the effects of those cure cycles on the resulting morphology, thermal properties, and rheology of the blends.

Preparation of hot-melt blends

Two types of samples were prepared. The first group was mixed and then frozen for use as stock in the differential scanning calorimetry (DSC), thermogravimetric analysis (TGA), and dynamic mechanical analysis (DMA) samples. This group of samples will be referred to as the 'uncured samples' because at the beginning of each test,

they had not had heat applied to them beyond the heat needed to mix them. The second group of samples was mixed in the same way as the uncured samples, but the samples were subsequently subjected to one of two cure cycles each capable of curing the BMI in the blend (assuming the BMI remained a separate phase in the mixture). Therefore, the second group of samples will be referred to as the 'cured' samples. Some of the cured samples were used for the additional thermal stability studies in which post-cures were later applied. The rest of the cured samples were cut and mounted as scanning electron microscopic (SEM) samples.

The preparation of uncured samples was relatively straightforward. For the RD-730 samples, the frozen RD-730 resin was weighed and placed in a preheated silicone mold, where it melted and took the form of the mold. For the Matrimid A/B samples, liquid DABA (component B of the Matrimid BMI) was weighed and placed in a beaker with a silicone oil bath at 150°C for 10 min while slowly adding the component A of the Matrimid A/B powder. To prepare the blended samples (also uncured), a similar procedure was followed except the desired amount of RD-730 was heated in a beaker before components B and A of Matrimid A/B were added. Samples were removed from the bath, cast in preheated (150°C) silicone molds in the shape of bars sized for DMA testing, and then quenched in a freezer to stop the reaction. The maximum ratio of RD-730 to Matrimid A/B that was possible to fabricate in blend form with this process was 40/60. At higher RD-730/Matrimid ratios, the mixture of RD-730 and Matrimid component B became too viscous before all the Matrimid component A powder could be added to the mixture. After mixing, all molds were covered with a silicone rubber plate to help eliminate the bubbles from the blends.

The cured samples were prepared with the same steps as the uncured samples but without quenching. After application of the silicone rubber plate, they were vacuum-bagged and cured (Figure 4). The cured samples were separated into two groups and each group was cured with a different cure cycle – either a long dwell cure cycle or a fast ramp cure cycle. The long dwell cure cycle consisted of:

Table 1. RD-730/Matrimid A/B blend compositions.

Blend ratio	RD-730 (g)	Matrimid A/B	
		Component B (g)	Component A (g)
RD-730	20	0	0
40/60 RD-730/ Matrimid	8	5.2	6.8
30/70 RD-730/ Matrimid	6	6.0	8.0
20/80 RD-730/ Matrimid	4	6.9	9.1
10/90 RD-730/ Matrimid	2	7.7	10.3
5/95 RD-730/ Matrimid	1	8.2	10.8
1/99 RD-730/ Matrimid	0.2	8.5	11.3
Matrimid	0	8.6	11.4

1. vacuum followed by 690 kPa autoclave pressure once heating began,
2. ramp rate at 2.8°C/min to 125°C,
3. hold for 4 h at 125°C,
4. ramp rate at 2.8°C/min to 204°C,
5. vent vacuum at 204°C,
6. hold for 4 h at 204°C, and
7. cool down to room temperature (RT) at 2.8°C/min.

The fast ramp cure cycle consisted of:

1. vacuum followed by 690 kPa autoclave pressure once heating began,
2. ramp rate at 2.8°C/min to 204°C,
3. hold for 4 h at 204°C, and
4. cool down to RT at 2.8°C/min.

Blends were made with weight fractions of RD-730 ranging from 1% to 40% (Table 1). A ratio of 43:57 parts by weight of component B to component A was used for the Matrimid A/B in all of the blends.

Thermal analysis and morphology characterization

Weight loss versus temperature was evaluated on the uncured resins and blends using a TA Instruments TGA model Q500. Small samples of approximately 25 mg were run using a ramp rate of 10°C/min to a final temperature of 1000°C in an air atmosphere. Thermal transitions of the uncured neat resins and blends were determined by TA Instruments model Q100 DSC. The measurement was performed by a sample mass of approximately 15 mg. Each sample was placed in a sealed aluminum pan and tested by a ramp rate at 10°C/min from RT to 400°C in a nitrogen atmosphere. The T_g of these same materials was determined using a TA instruments ARES DMA in an air

atmosphere. The instrument was run using the 25 mm parallel plate geometry with a frequency of 1 Hz. The dynamic ramp tests consisted of a ramp rate at 5°C/min to 400°C, and the sample was cooled down at 5°C/min from 400°C to RT, while a measurement was taken every 10s. The T_g was determined using the midpoint temperature of the highest value of $\tan \delta$ from the cooling portion of the $\tan \delta$ versus temperature curve.

For the cured samples, small sections were cut, polished, and sputter-coated with carbon. The cross-sections were examined with a Quanta 600F SEM to observe the amount and distribution of phase separation – when it occurred. This was repeated on several cross-sections of each sample to identify a representative average amount of phase separation. Using the same instrument in energy dispersive x-ray (EDX) mode, selected areas of the samples were interrogated to determine the elemental composition in order to determine which constituent (Matrimid A/B or RD-730) was in each phase. DMA tests were also performed on the cured samples. Torsion mode was used on specimens with dimensions of $30 \times 11 \times 2 \text{ mm}^3$ ($L \times W \times T$). The applied strain amplitude was 0.3% at a deformation frequency of 1 Hz. The procedure consisted of:

1. heat at 5°C/min from RT to 250°C,
2. hold for 4 h (first post-cure studied),
3. cool down from 250°C to 40°C at a rate of 5°C/min,
4. heat from 40°C to 300°C at a rate of 5°C/min,
5. hold for 4 h (second post-cure studied),
6. cool down from 300°C to RT at a rate of 5°C/min.

Results and discussion

Thermal properties

To establish a baseline, first, the weight loss of the uncured RD-730/Matrimid A/B blends was measured. The results are shown in Figure 5(a) as a function of temperature for a TGA heating rate of 10°C/min. RD-730 had an initial weight loss at approximately 110°C before undergoing a pyrolytic ceramic conversion reaction that was essentially completed at 700°C. The observed 62% char yield for RD-730 is reasonably close to the 67% char yield reported in Starfire RD-730 Product Brochure.¹⁹ Matrimid A/B had a small initial weight loss at approximately 200°C, followed by a much larger weight loss that began around 400°C, and continued until full decomposition of the polymer at 650°C. Thus, the cure ranges of the RD-730 and Matrimid were overlapped. This was not ideal but was a necessary compromise due to the limited number of preceramic polymers available with the desired chemical structure and processing properties. The TGA profiles of the blends (Figure 5(b)) generally resembled the TGA profile of the Matrimid A/B resin but were shifted upward toward the RD-730 curve with increasing RD-730 content. The mass retained above 800°C increased proportionally with the

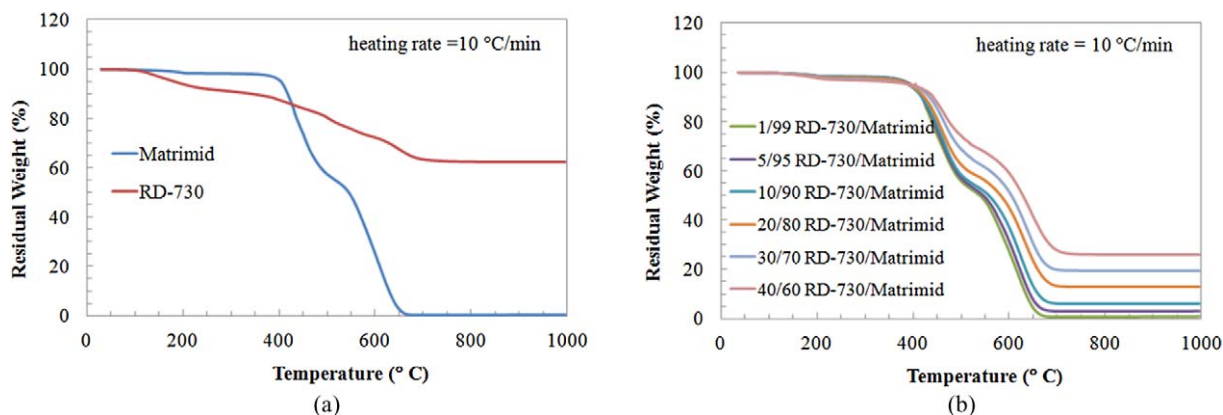


Figure 5. Weight loss of (a) the uncured pure resins and (b) the uncured blends.

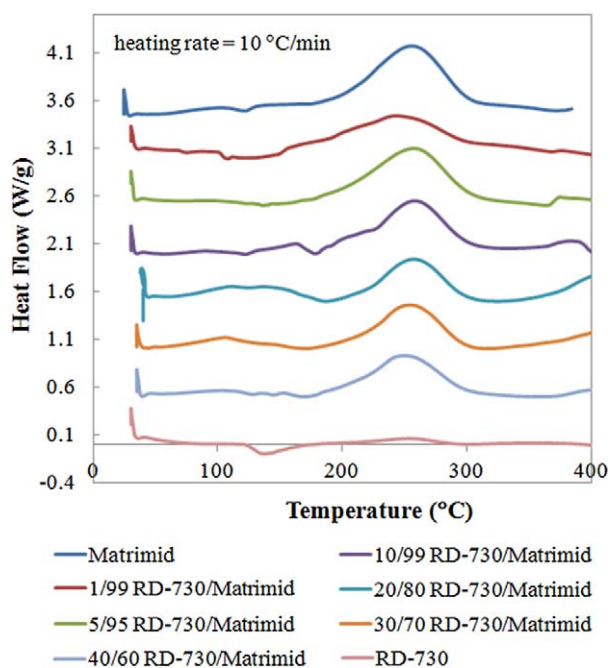


Figure 6. DSC curves of uncured RD-730, Matrimid A/B, and the blends.

DSC: differential scanning calorimetry.

RD-730 content in the blend. To be clear, it was not expected that the blends would be cured to 800°C or higher when in service in a hybrid application. The temperature range for the weight loss study was chosen to establish whether the decomposition temperature of any of the blends was greater than the decomposition temperature of the Matrimid. Unfortunately, the data in Figure 5(b) imply that degradation occurred as if the Matrimid A/B and the RD-730 were present in the same ratio throughout the heating process as in the original samples. This, in turn, is an indicator that a chemical reaction between the Matrimid A/B and RD-730 did not occur to any significant extent (at least for a heating profile of RT to 1000°C at a rate of 10°C/min).

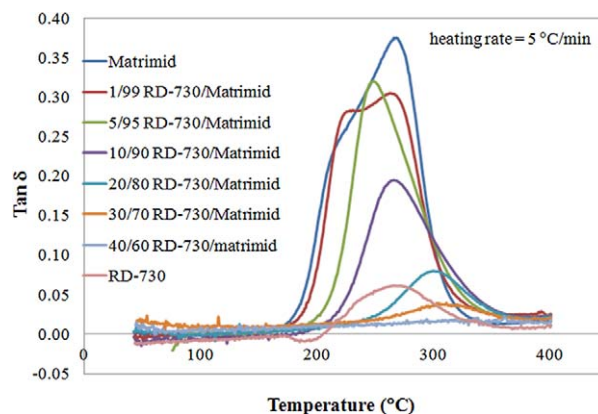


Figure 7. Tan δ versus temperature for RD-730, Matrimid A/B, and the blends from cooling traces.

DSC traces from RT to 400°C of the uncured samples are shown in Figure 6. All the samples had a small peak at 150°C indicating the onset of curing, and they also had a broad exothermic peak at 250°C presumably indicating the cross-linking. Surprisingly, this was even true for the pure RD-730 sample. The coincidence of the peaks for the pure RD-730 and pure Matrimid A/B samples was unfortunate because this made it unlikely that a shift in the 250°C peak would occur with increasing RD-730 even if the two constituents reacted. However, no new peak – e.g. a peak that might correspond to the reaction that was hoped for between the double bond of the imide in Matrimid A/B and the reactive groups of the pre-RD-730 – was apparent in the blends. This is not conclusive evidence of the absence of a chemical reaction between the two species but it is consistent with no reaction. The intention was to tabulate the T_g as a function of RD-730 concentration from the DSC data in Figure 6 (in this case, it would likely have been a constant versus RD-730 concentration) in comparison with the T_g from the data in Figure 7 from the DMA tests on the same samples, but the peaks were too broad to determine T_g with an adequate accuracy.

Table 2. T_g values of RD-730, Matrimid A/B, and their blends from cooling traces.

Composition	T_g ($^{\circ}\text{C}$)
Matrimid A/B	271
1/99 RD-730/Matrimid	n/a
5/95 RD-730/Matrimid	252
10/90 RD-730/Matrimid	270
20/80 RD-730/Matrimid	300
30/70 RD-730/Matrimid	306
40/60 RD-730/Matrimid	n/a
RD-730	264

The T_g s of the uncured pure resins and blends were determined by DMA. The $\tan \delta$ versus temperature curves are shown in Figure 7 and the T_g for each composition is tabulated in Table 2. At low RD-730 weight fractions, the T_g of the blends remained at 270 $^{\circ}\text{C}$ or below. However, a significant increase in T_g to 300 $^{\circ}\text{C}$ was observed at 20 wt% and 30 wt% of RD-730 (the T_g of the 40 wt% RD-730 blend could not be determined). The T_g of a polymer in immiscible blends would not be expected to change with concentration ratio as long as the lower T_g material is the matrix of the blend, whereas in miscible blends, the T_g commonly takes on a value intermediate to the T_g of the components. Therefore, the increase in T_g with increasing RD-730 content was somewhat surprising since the blends were thought to be immiscible based on the DSC and TGA results. Another circumstance that can cause a shift in the T_g of the components in a blend is a difference in thermal expansion coefficients between the phases of the blend. This may be a mechanism contributing to the increase in T_g . Finally, the presence of two distinct peaks in the 1% RD-730 data was a significant anomaly. The Matrimid curve has a slight shoulder, the 1% curve has a distinct second peak, and the 5% curve has no trace of a shoulder. A cause for this was not apparent, but it is consistent with the other results. The DSC data in Figure 6 contains a similar trend. The peak at 250 $^{\circ}\text{C}$ is well defined in the Matrimid plot, and the same peak broadens significantly in the 1% plot and returns to a defined peak in the 5% plot.

Morphology

As mentioned above, for the cured samples, two cure cycles were investigated – a long dwell cure cycle and a fast ramp cure cycle. The morphology of the blends after curing was examined by a SEM.

Long dwell cure cycle

Figure 8 shows the representative cross-sectional morphologies of the blends at each composition after curing with the long dwell cure cycle. The images are oriented, so that the bottom of the image corresponds to where the sample

was in contact with the bottom of the mold. A two-phase morphology was observed. The light phase in the image represents RD-730 and the dark phase is the Matrimid A/B matrix based on the small amount of light phase in the 1% RD-730 sample and the increasing amount of light phase present as the RD-730 content was increased. At low-weight fractions of RD-730 (1% and 5%), the RD-730 was dispersed as fine spheres in the Matrimid A/B matrix. As the weight fraction of RD-730 increased, the number of dispersed RD-730 droplets (both spheres and more complex irregular shapes) increased and the RD-730 droplets coalesced to produce much larger domains. A gradient phase morphology was apparent in the 10/90 and 20/80 RD-730/Matrimid A/B blends and to a smaller extent in the 30/70 blend. The size of the RD-730 droplets can be seen to increase gradually when viewing locations that vary from the bottom to the top surface. The overall concentration of the RD-730 changed in a similar manner. The observed graded morphology may have implications for the potential of making graded regions in hybrids materials. In this case, the grading is produced as a result of gravity. Therefore, in complex-shaped parts or parts that include a dense fabric of reinforcing fibers, a different approach to grading would be necessary.

Elemental mappings using SEM in EDX mode are shown in Figure 9. A representative spherical shaped RD-730 inclusion is shown at much higher magnification (the inclusion is approximately 20 μm in diameter). It is clear that the RD-730 inclusion contained hundreds of smaller spheres. Since the smaller spheres contained carbon but did not contain silicon or oxygen, it is believed that they were Matrimid A/B, that is, each larger RD-730 inclusion was actually a phase-separated region of both RD-730 and Matrimid A/B that was phase-inverted. Similarly, in the region surrounding the large spherical RD-730 inclusion, there was no silicon – which corroborates the previous results that indicated that the RD-730 did not react with the Matrimid as had been hoped.

Fast ramp cure cycle

The fast ramp cure cycle samples were also imaged to determine the influence of cure profile variations on the morphology of the blends. It was expected that the size of RD-730 inclusions would be smaller after the fast ramp cycle due to the elimination of the isothermal hold at 125 $^{\circ}\text{C}$ for 4 h. It was thought that at a faster rate of curing, the dispersed RD-730 domains would have less time to coalesce when the blend was at a low viscosity. Figure 10 shows the representative low-magnification images of the morphologies of the blends at various compositions. Phase separation was observed similar to the phase separation seen in the long dwell samples and a gradient phase morphology was observed in the 10/90 and 20/80 samples. It is apparent, from a comparison of Figures 8 and 10, that the cure cycles

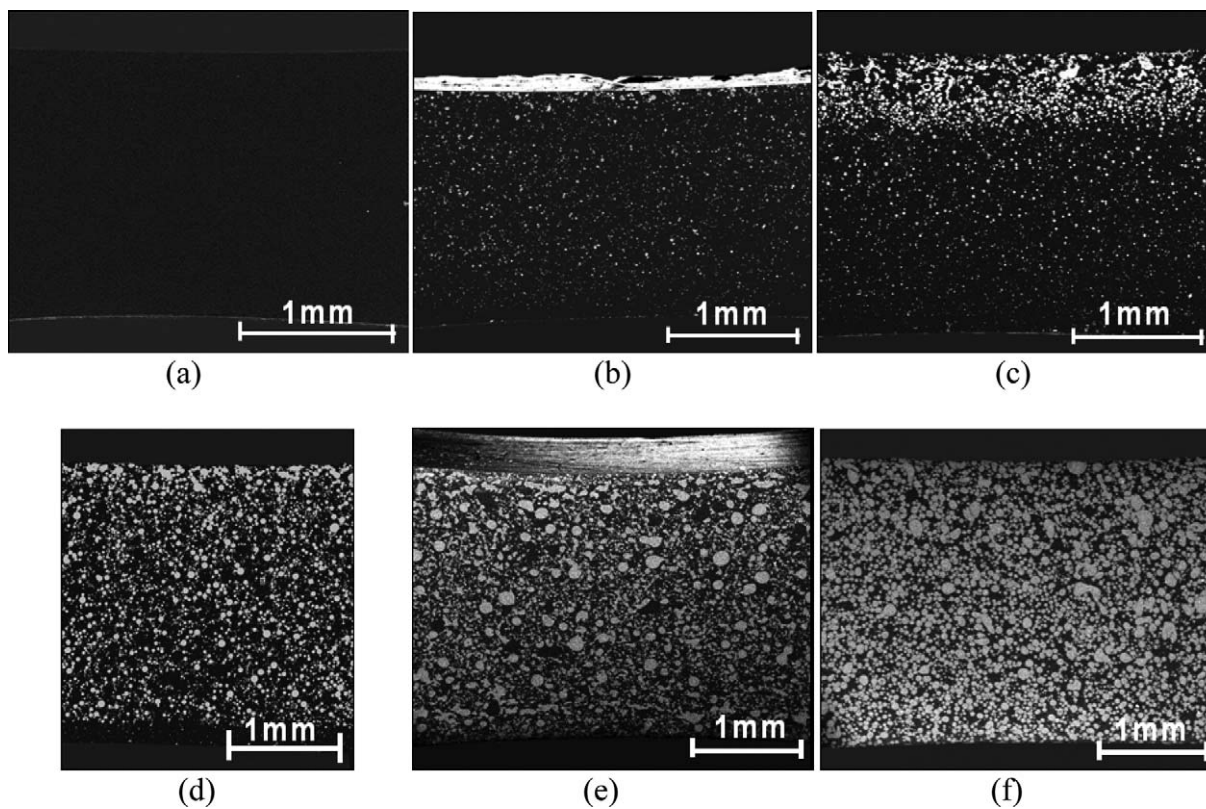


Figure 8. Low magnification SEM images of the blends after curing with the long dwell cure cycle: (a) 1/99, (b) 5/95, (c) 10/90, (d) 20/80, (e) 30/70, and (f) (40/60).
SEM: scanning electron microscopy.

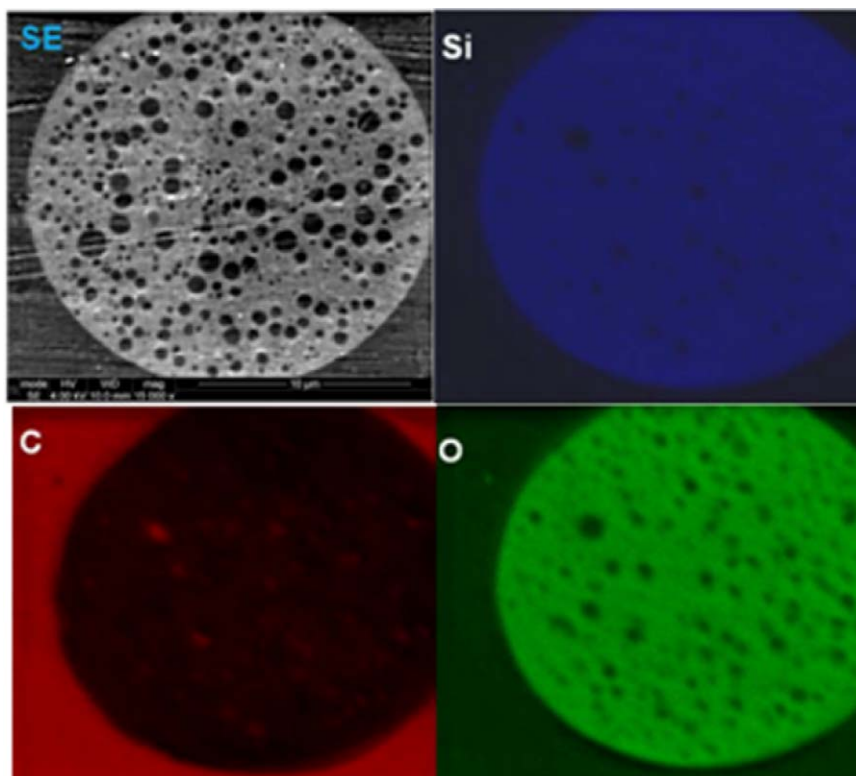


Figure 9. An SEM image (top left) and elemental maps for Si (blue), C (red), and O (green) of a representative RD-730 domain.
SEM: scanning electron microscopy.

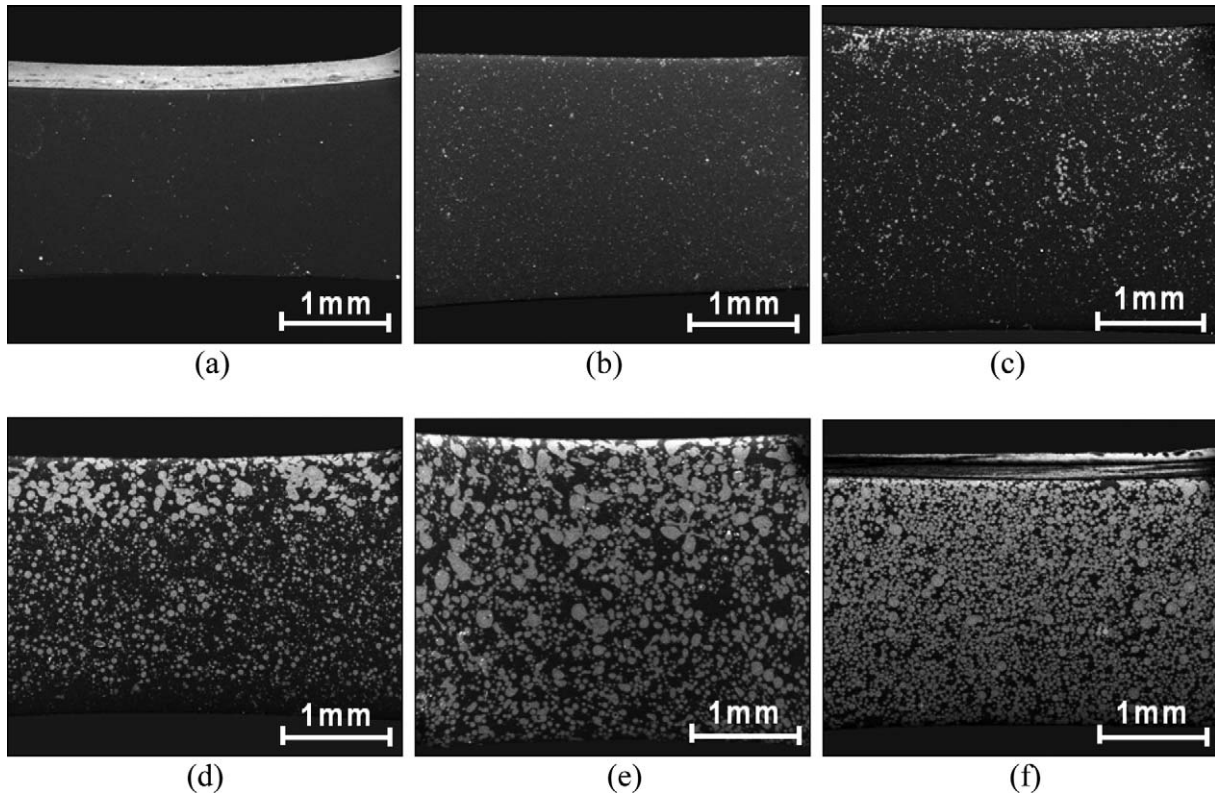


Figure 10. Low magnification SEM images of the blends after curing with the fast ramp cure cycle: (a) 1/99, (b) 5/95, (c) 10/90, (d) 20/80, (e) 30/70, and (f) 40/60. SEM: scanning electron microscopy.

used in this study had only a minor impact on the morphology of the blends. This is further corroborated by the SEM images shown in Table 3 of the cured blends at a higher magnification (full image is roughly 0.3 mm across vs. 3 mm across for the images shown in Figures 8 and 10). Strong similarities between the morphologies were apparent except for the 30/70 composition that had noticeably more clustering of the RD-730 domains in case of the fast ramp-cured specimen.

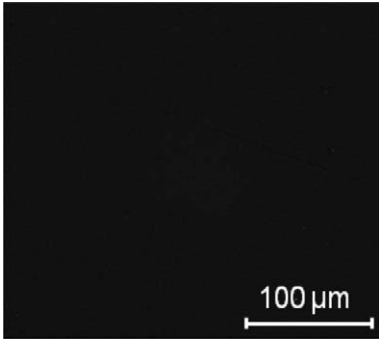
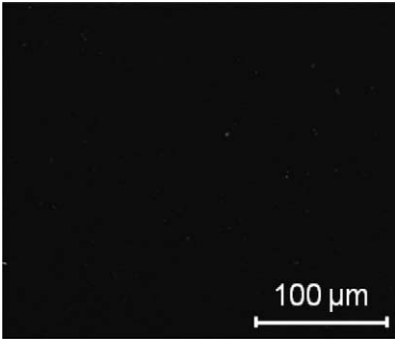
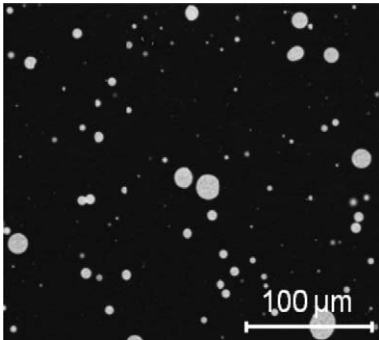
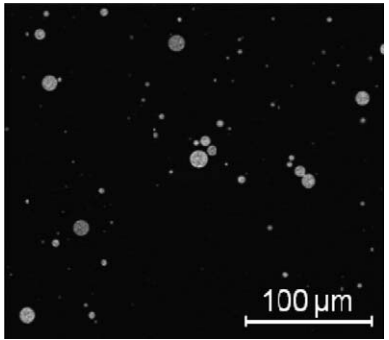
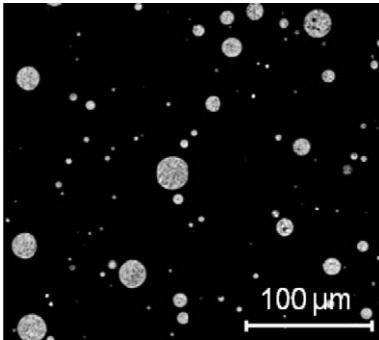
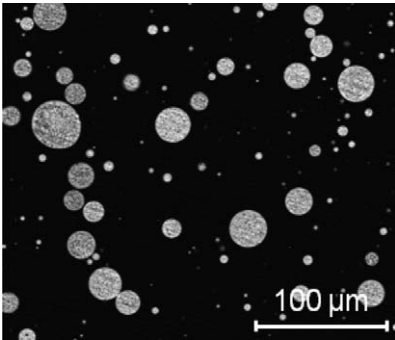
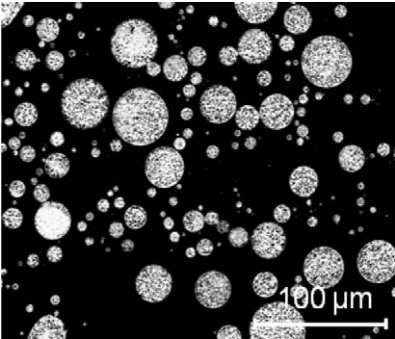
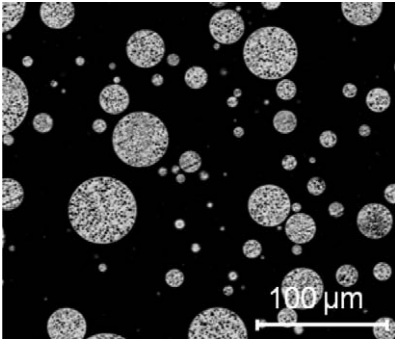
Glass transition temperature

The choice of processing parameters for the T_g study took careful consideration. For the group of the cured samples used for the morphology study, the cure cycles chosen were sufficient to lock in the morphology. Furthermore, post-curing would not have altered the results; so they were not post-cured. However, for mechanical properties and T_g , a post-cure can make a very significant difference. In choosing a combination of cure cycle and post-cure for the samples to be used in DMA testing, the ultimate use of these blends was kept in mind, which was imagined to be the matrix of a fiber-reinforced transition layer between a PMC and a CMC. A PMC with a matrix such as Matrimid A/B would typically be cured in an autoclave with a cycle that

would be a compromise of the fast ramp cure cycle and the long dwell cure cycle. Then the cure would be followed by a post-cure in an oven to a temperature in the neighborhood of the expected service temperature of the composite part. The post-cure would normally drive up the T_g and improve thermal stability at the higher service-temperature. Beyond a post-cure at 250°C–300°C, there is little more that could be done to the Matrimid A/B to complete its cure or increase its use-temperature without charring or degrading it to some extent. Since the blends had already been shown to be phase separated, the Matrimid A/B cure temperature limit of 300°C was most likely also the cure temperature limit for the blends. Therefore, the DMA study on the cured samples was conducted on the blend samples cured (either with the fast ramp or long dwell cycle) and then post-cured at either 250°C or 300°C.

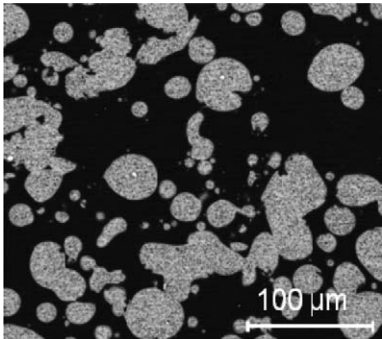
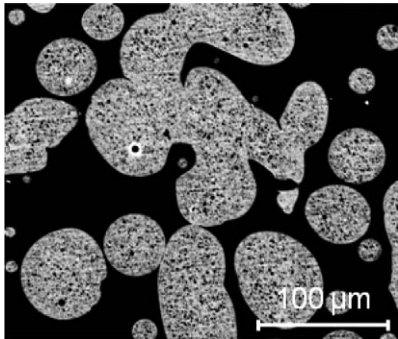
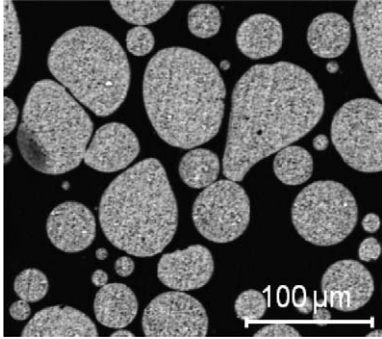
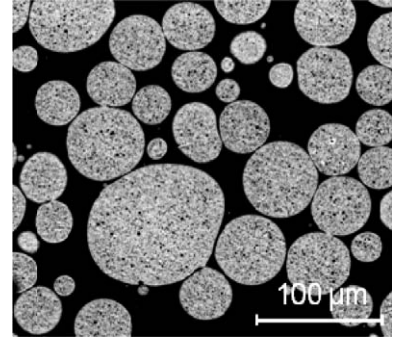
Plots of $\tan \delta$ as a function of temperature from DMA cooling traces for the blends are shown in Figure 11 for the samples subjected to the long dwell cure cycle. Figure 11(a) shows results for samples post-cured for 4 h at 250°C and Figure 11(b) shows results for samples post-cured for 4 h at 250°C followed by 4 h at 300°C. For the 250°C post-cure sample, the $\tan \delta$ curve of RD-730 had a very broad peak with a maximum at 180°C while the maximum for Matrimid A/B was located at 250°C. The

Table 3. Comparison of the morphology of the RD-730/Matrimid blends after long dwell and fast ramp curing.

RD-730/Matrimid weight ratio	Long dwell cure cycle	Fast ramp cure cycle
1/99		
5/95		
10/90		
20/80		

(continued)

Table 3. (continued)

RD-730/Matrimid weight ratio	Long dwell cure cycle	Fast ramp cure cycle
30/70		
40/60		

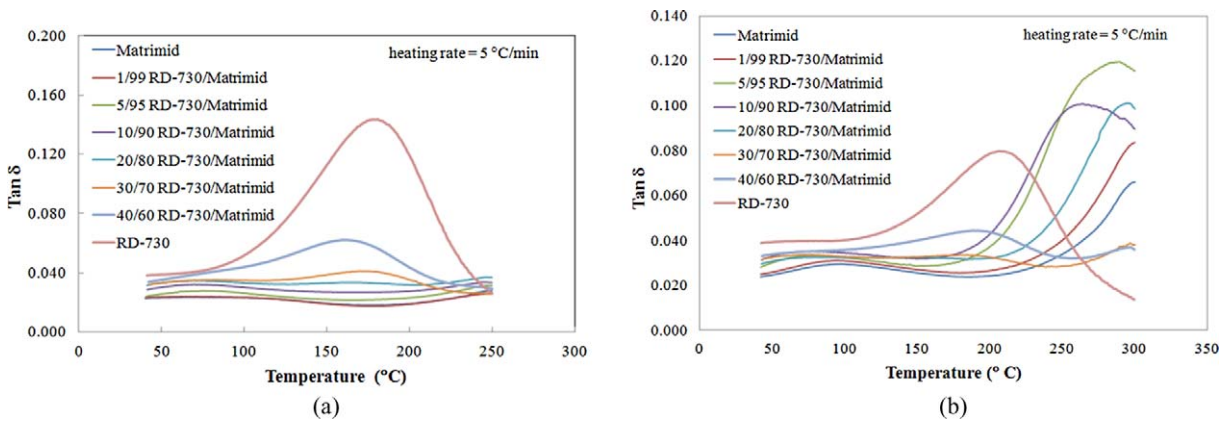


Figure 11. $\tan \delta$ versus temperature of the pure resins and blends after the long dwell cure followed by: (a) a post-cure for 4 h at 250°C or (b) a post-cure for 4 h at 250°C plus 4 h at 300°C.

behavior of the blends was found to depend on the composition ratio. At low-weight fractions of RD-730 (1–10%), the location of the peak was very close to the 250°C of the Matrimid A/B matrix, whereas at higher weight fractions of RD-730, the peak was much nearer to the 180°C peak of the RD-730. Only one maximum was observed in this temperature range (with the possible exception of the 20/80 sample), even though two phases were present in the blends. An additional post-cure at 300°C for 4 h, resulted in

advancing the T_g for all the samples (Figure 11(b)). Trends were similar to the 250°C post-cured samples. High weight fractions of RD-730 (30–40%) had peaks near the 205°C peak, and as the weight fraction reduced, the location of the peak moved closer to the 300°C peak of the Matrimid A/B. Figure 12 shows nearly identical results for the fast ramp samples compared with the results for the long dwell samples shown in Figure 11. Modifying the base cure cycle had no significant effect on the

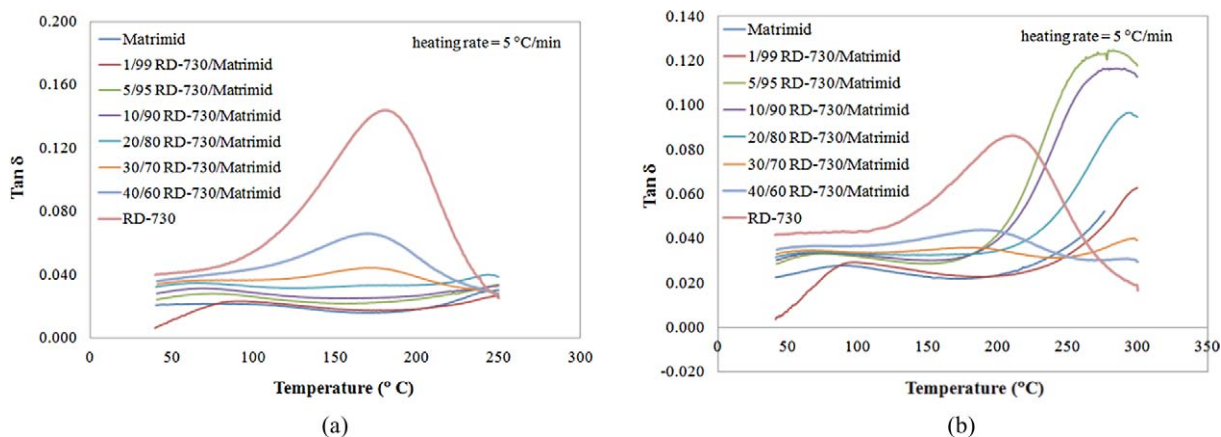


Figure 12. $\tan \delta$ versus temperature of the pure resins and blends after the fast ramp cure followed by: (a) a post-cure for 4 h at 250°C or (b) a post-cure for 4 h at 250°C plus 4 h at 300°C.

Table 4. T_g values of the pure resins and the blends as a function of post-cure conditions.

Sample composition	T_g (°C) fast ramp cure		T_g (°C) long dwell cure	
	PC: 4 h at 250°C	PC: 4 h at 250°C 4 h at 300°C	PC: 4 h at 250°C	PC: 4 h at 250°C 4 h at 300°C
Matrimid	250	300	250	300
1/99 RD-730/Matrimid	250	300	250	300
5/95 RD-730/Matrimid	250	282	247	288
10/90 RD-730/Matrimid	248	283	246	264
20/80 RD-730/Matrimid	243	295	246	295
30/70 RD-730/Matrimid	177	295	172	298
40/60 RD-730/Matrimid	170	190	172	190
RD-730	181	210	180	208

PC: post-cured.

behavior of the pure components and the blends, which is consistent with the morphological observations. T_g values derived from the data in Figures 11 and 12 are listed in Table 4.

A clear drawback to blending these two resins (other than the fact that they did not chemically react to form a new material) is that for the cure cycle/post-cure combinations that were appropriate for the Matrimid A/B, the RD-730 responded with a significantly lower T_g than the Matrimid A/B. Consequently, not only is the blend not better than the Matrimid A/B by itself but also it is actually a poorer material in terms of temperature performance. It is still possible that the CTE and/or stiffness of one or more of the blends could be intermediate to the CTE and/or stiffness of the RD-730 and Matrimid A/B, but this would be achieved at a cost of at least 90°C in reduced temperature capability. On the other hand, the data in Figure 7 and Table 2 hint at a resolution. As can be seen in Figure 7, a relatively short excursion to 400°C significantly drove up the T_g of the RD-730 to 264°C, which is much closer to the maximum achievable T_g of the Matrimid with a long 300°C post-cure sample. While the Matrimid A/B could not be

used long-term at 400°C without major degradation, it may be possible to add a relatively short period at 400°C to the cure cycle as was done for the uncured blend samples. The data suggest that this could produce a hybrid material with the service temperature of the Matrimid. This also highlights a further point which is that a higher temperature polyimide such as AFR-PE-4 may be a better choice than Matrimid A/B for future work in this area.²⁴ Cost and processing complexity would be added when working with AFR-PE-4, but the RD-730 was quite responsive to time spent at 400°C to increase its T_g so it may be worthwhile to make the switch.

Conclusions

Blends of the RD-730 and Matrimid A/B with various compositions were successfully fabricated by hot-melt mixing followed by casting and curing. The effects of composition and cure cycle variations on the morphology and thermal properties of the blends were investigated using SEM, DSC, TGA, and DMA. Several conclusions were made based on the test results.

- Blends of the RD-730 with Matrimid A/B were found to have a two-phase morphology in which RD-730 was primarily dispersed as particles within a Matrimid A/B matrix.
- As the weight fraction of RD-730 was increased from 1% to 40%, the dispersed RD-730 inclusions increased from an average size of 3 μm to more than 40 μm and each of the larger RD-730 inclusions in the blends enclosed a distribution of much smaller Matrimid A/B spheres approximately 1 μm in diameter.
- A gradient phase morphology was consistently fabricated at intermediate RD-730 weight fractions (10–30 wt%). This spatially varying morphology may be useful for a transition layer in a hybrid structure in which a ceramic layer needs to be connected to a polymer or a PMC layer. However, it should be noted in the context of PMC/CMC hybrids that the potential for producing these gradients in the presence of a dense field of reinforcing fibers could be difficult to achieve.
- Changing the cure cycle to reduce the period of time in which the RD-730 had peak mobility had very small impact on the morphology and T_g of the blends.
- Finally, the DMA testing results indicated that it may be possible to drive the T_g of the RD-730 component in the blend up to near the maximum achievable T_g of the Matrimid A/B with a short hold at 400°C, but the hold must be kept brief enough to prevent the degradation of the Matrimid A/B. Alternatively, a switch to a higher temperature polyimide appeared promising.

In summary, a wide range of experiments showed that altering the processing cycle did not lead to a significantly increased miscibility. This is unfortunate, since an increased miscibility would likely have been a good indication that the RD-730 and Matrimid A/B were chemically reacting or mixing sufficiently to potentially result in a new material with a stiffness, temperature capability, and CTE in the property space between that of RD-730 and Matrimid A/B. As a result, this article serves as a motivation to move to more radical approaches in the fabrication of a BMI/pre-ceramic polymer hybrid. In the follow-on article to this work,²⁵ the success achieved in using chemical compatibilizers added as a third constituent to take advantage of the differences in polarization of the two base constituents in order to make the two resins more miscible is explored in detail. The current article also constitutes a documentation of the baseline for the materials used in the follow-on article's compatibilizer study.

Acknowledgements

The authors thank Mr Sean Gretzinger (Southern Ohio Research Council on Higher Education) for his help in sample preparation. The authors also gratefully acknowledge discussions and input on thermal analysis of the RD-730/Matrimid A/B blends from Dr

William Lee (University of Dayton Research Institute), Dr Venkat Narayanan (UDRI), and Dr David Wang (UES).

Funding

Direct funding for this work was provided by the Air Force Research Laboratory through funding on contract FA8650-05-D-5052.

References

1. KICKELBICK G. Introduction to hybrid materials. In: KICKELBICK G (ed) *Hybrid materials synthesis, characterization, and application*. Weinheim, Germany: Wiley-VCH, Verlag GmbH; 2006, pp. 1–48.
2. Parthasarathy TA, Jefferson GJ and Kerans RJ. Analytical evaluation of ceramic design concepts for optimized structural performance. *Mater Sci Eng A* 2007; **459**: 60–68.
3. Jefferson GJ, Parthasarathy TA and Kerans RJ. Materials design of hybrid ceramic composites for hot structures. In: *Proceedings of the 35th international SAMPE technical conference*, Dayton, OH, 28 Sep–2 Oct, 2003.
4. Ashby M. Hybrid materials to expand the boundaries of material-property space. *J Am Ceram Soc* 2011; **94**(S1): s3–s14.
5. Glass DE. Ceramic matrix composites (CMC) thermal protection systems (TPS) and hot structures for hypersonic vehicles. In: *Proceedings of the 15th AIAA international space planes and hypersonic systems and technologies conference*, Dayton, OH, 28 Apr–1 May, 2008.; paper AIAA 2008-2682.
6. Shabana YM and Noda N. Thermo-elasto-plastic stresses in functionally graded materials subjected to thermal loading taking residual stresses of the fabrication process into consideration. *Composites B* 2001; **32**(2): 111–121.
7. Birman V and Byrd LW. Modeling and analysis of functionally graded materials and structures. *Appl Mech Rev* 2007; **60**: 195–216.
8. Brown J, Allred R, Duncan T, et al. *Hybrid composite article and missile components and their fabrication*. Patent No. 5979826, USA, 1999.
9. Beckley DA and Stites J. *Silicone composite materials having high temperature resistance*. Patent No. 16751, EP, 1995.
10. Wilson D, Beckley D and Koo JH. Development of silicone matrix-based advanced composites for thermal protection. *High Perform Polym* 1994; **6**(2): 165–181.
11. Burns GT, Taylor RB, Xu Y, et al. High-temperature chemistry of the conversion of siloxanes to silicon carbide. *Chem Mater* 1992; **4**: 1313–1323.
12. Elias L, Fenouillot F, Majeste JC, et al. Morphology and rheology of immiscible polymer blends filled with silica nanoparticles. *Polymer* 2007; **48**: 6029–6040.
13. Takahashi T, Münstedt H, Columbo P, et al. Thermal evolution of a silicone resin/polyurethane blend from preceramic to ceramic foam. *J Mat Sci* 2001; **36**: 1627–1639.
14. Laine R and Babonneau F. Pre-ceramic polymer routes to silicon carbide. *Chem Mater* 1993; **5**: 260–279.
15. Bouillon E, Langlais F, Pailler R, et al. Conversion mechanisms of a polycarbosilane precursor into a SiC-based ceramic material. *J Mater Sci* 1991; **26**: 1333–1345.

16. Leonard V, Interrante V, Whitmarsh CW, et al. High yield polycarbosilane, precursors to stoichiometric SiC, synthesis, pyrolysis, and application. *MRS Proceedings* 1994; **346**: 595.
17. Bernardo E, Colombo P and Hampshire S. Advanced ceramics from a preceramic polymer and nano-fillers. *J Eur Ceram Soc* 2009; **29**: 843–849.
18. Colombo P, Mera G, Riedel R, et al. Polymer derived ceramics: 40 years of research and innovation in advanced ceramics. *J Am Ceram Soc* 2010; **93**(7): 1805–1837.
19. *Starfire RD-730 Product Brochure*, rev. 2, 2007. Available at: <http://starfiresystems.com/docs/ceramics-forming-polymers/SMP-730.pdf>. Accessed on 29 November 2012.
20. *Material Safety Data Sheet Starfire RD-730*, rev. 2, 2009. Starfire Systems, Schenectady, NY, USA.
21. Brown JM, Srinivasan S, Rau A, et al. Production of controlled networks and morphologies in toughened thermosetting resins using real-time, *in situ* cure monitoring. *Polymer* 1996; **37**(9): 1691–1696.
22. Brown JM, Putthanarat S, Trejo R, et al. Preceramic polymer for gradient organic-inorganic morphologies. *SAMPE Proceedings* 2010.
23. Sabzevari SM, Alavi-Soltani S, Koushyar H, et al. Modification of time-temperature-transformation diagram to obtain a comprehensive cure map for polymer composites. In: *Proceedings of the 41st international SAMPE technical conference*, Wichita, Kansas, USA, October 19–22, 2009.
24. Whitley K and Collins T. Mechanical properties of T650-35/AFR-PE-4 at elevated temperatures for lightweight aeroshell designs. In: *Proceedings of the 47th AIAA/ASME/ASCE/AHS/ASC structures, structural dynamics, and materials conference* Newport, Rhode Island, May 1-4, 2006. paper AIAA 2006–2202.
25. McKellar R, Venkat N, Safriet S, et al. Bismaleimide/preceramic polymer blends for hybrid material transition regions, Part 2: incorporating compatibilizers. *High Perform Polym*, in this issue.